VALIDATION OF MONTE CARLO YIELD FUNCTION OF A SEMI-LEADED NEUTRON MONITOR USING LATITUDE SURVEY DATA IN 2019 AND 2020

A. Seripienlert[a], W. Nuntiyakul[b], S. Khamphakdee[b], P.-S. Mangeard[c], A. Sáiz[d], D. Ruffolo[d], P. Evenson[c], K. Fongsamut[b], P. Jiang[e], P. Chuanraksasat[a], K. Munakata[f], J. Madsen[g], B. Soonthornthum[a], S. Komonjinda[b]

[a]National Astronomical Research Institute of Thailand (NARIT), Thailand [b]Chiang Mai University, Thailand [c]University of Delaware, USA [d]Mahidol University, Thailand
[e]Polar Research Institute of China, China [f]Shinshu University, Japan [g]University of Wisconsin-Madison, USA

ABSTRACT

A neutron monitor (NM) is a ground- (or sea-) based detector of the flux of cosmic ray particles in space. The high-energy cosmic rays in the GeV primary range interact in the upper atmosphere, producing a cascade of subatomic particles, some of which reach Earth's surface. A neutron monitor is mostly sensitive to the neutron component of the atmospheric cascade. These neutrons can then be detected by induced nuclear fission of ^{10}B in a $^{10}BF_3$ gas proportional counter. The Changvan neutron monitor is a portable neutron monitor assembled in Thailand and housed in a standard insulated shipping container to conduct long-term research in polar regions. There are three proportional counters housed in the insulated shipping container, but the central counter lacks the lead producer. We performed a Monte Carlo Simulation for the yield function of the Changvan monitor to primary particles. We validated our preliminary yield function by comparing count rates from simulation with actual data. We found that the maximum difference of the unleaded/leaded count rate ratio between simulation and experimental data was less than 8%. This leads to a promising yield function that can be used to determine the spectral index of relativistic solar ions with a single detector.

MONTE CARLO SIMULATION

Our Monte Carlo simulations used FLUKA (FLUKtuierende KAskade), version 4.1-1, which is an open-source particle physics package (https://fluka.cern/), [13, 14]. DPMJET hadron interaction models is using [15, 16]. The FLUKA simulation process used in this work can be divided into two parts: Atmospheric simulation and Detector simulation. Analysis of simulated yield function and count rates are done after completing the FLUKA simulation.

ATMOSPHERIC SIMULATION

We created an atmospheric profile using data from the Global Data Assimilation System (GDAS) and NRLMSISE-00. We assumed a spherical atmosphere for the simulation, following the method described in [5] for the Hobart atmosphere in this work. We simulated isotropic primary particles with rigidity ranges from 1 GV to 200 GV; 1,000,000 events for each species of primary cosmic rays. These events produced secondary cosmic rays totaling 1,299,064 particles (136,508 neutrons, 13,486 protons, and 1,149,070 muons). These secondary cosmic rays are stored in libraries for use in the detector simulation in the next step.

DETECTOR SIMULATION

Here, we use the detector geometry made with Flair 3.1 [8] shown in Figure 1. The geometry includes the Changvan monitor and structure surroundings provided by [17]. The container is placed on *Xuelong* icebreaker. We place seawater beneath the ship's entire lower half-spherical geometry. Secondary particles from the Libraries are chosen randomly and injected uniformly above the detector. We simulate 100,000,000 events for neutrons and protons and 25,000,000 events for muons. We applied deadtime 20 μs for all three tubes in the simulation. The results of the simulation are discussed in the next section.

REFERENCES

[1] Hatton, C.J. & H. Carmichael (1964), Can. J. Phys., 42, 2443–2472

[2] Nuntiyakul, W., Mangeard, P.-S., Ruffolo, D. et al (2020), J. Geophys. Res. Space Phys., 125, e27304

[3] Bieber, J. W., & Evenson, P. (1991), In Proc. of the 22 ICRC, 3, 129–132

[4] Caballero-Lopez, R.A., & Moraal, H. (2012), J. Geophys. Res., 117, A12103

[5] Mangeard, P.-S., Ruffolo, D., Sáiz, A. et al (2016), J. Geophys. Res. Space Phys., 121, 7435–7448

[6] Mangeard, P.-S., Ruffolo, D., Sáiz, A. et al (2016), J. Geophys. Res. Space Phys., 121, 11,620–11,636

[7] Banglieng, C., et al. (2020), Astrophys. J., 890, 21

[8] V. Vlachoudis, "FLAIR: A Powerful But User Friendly Graphical Interface For FLUKA", in Proc. Int. Conf. on Mathematics, Computational Methods & Reactor Physics (M&C 2009), Saratoga Springs, New York, 2009.

[9] Nuntiyakul, W., P. Evenson, D. Ruffolo et al (2014), Astrophys J., 795, 11

[10] Lin, Z., J.W. Bieber, P. Evenson et al (1995), J. Geophys. Res., 100, 23,543–23,550

[11] Bieber, J.W. & J. Clem (1997), In Proc. of the 25 ICRC, 2, 389–392

[12] Clem, J., J. W. Bieber, P. Evenson (1997), J. Geophys. Res., 102, 26,919–26,926

[13] G. Battistoni, T. Boehlen, F. Cerutti et al. (2015), Ann. Nucl. Energy, 82, 10-18.

[14] T.T. Bohlen, F. Cerutti, M.P.W. Chin et al. (2014), Nucl. Data Sheets, 120, 211-214.

[15] S. Roesler, R. Engel, J. Ranft et al. (2001), Springer-Verlag Berlin, 1033-1038.

[16] A. Fedynitch, PhD Thesis, https://cds.cern.ch/record/2231593/files/CERN-THESIS-2015-371.pdf

[17] Fongsamut K., P., Jiang, W., Nuntiyakul et al. (2021), J. Phys Conf. Ser., 1719, 012004

[18] Usoskin I.G., A., Gil, G.A., Kovaltsov et al. (2017), J. Geophys. Res. Space Phys., 122, 3875–3887

[19] Vos, E.E. & M. S. Potgieter (2015), Astrophys. J., 815, 119

LATITUDE SURVEY

CHANGVAN NEUTRON MONITOR

We built a mobile neutron monitor housed in a shipping container, nicknamed the "Changvan." We mounted the Changvan on the Chinese icebreaker *Xuelong* for two voyages between Shanghai, China, and Zhongshan station in Antarctica during 2019 and 2020 survey years. The Changvan neutron monitor contains three $^{10}BF_3$ proportional counters. The center counter lacks its own lead producer but has lead on either side, so we call this a semi-leaded 3NM64. Three square plywood segments with holes in the center are used to hold the center counter at the correct spacing. The thickness of each plywood segment is 1.5 cm. The two outer counters include the ring-shaped lead producer, as in the standard design for the NM64.
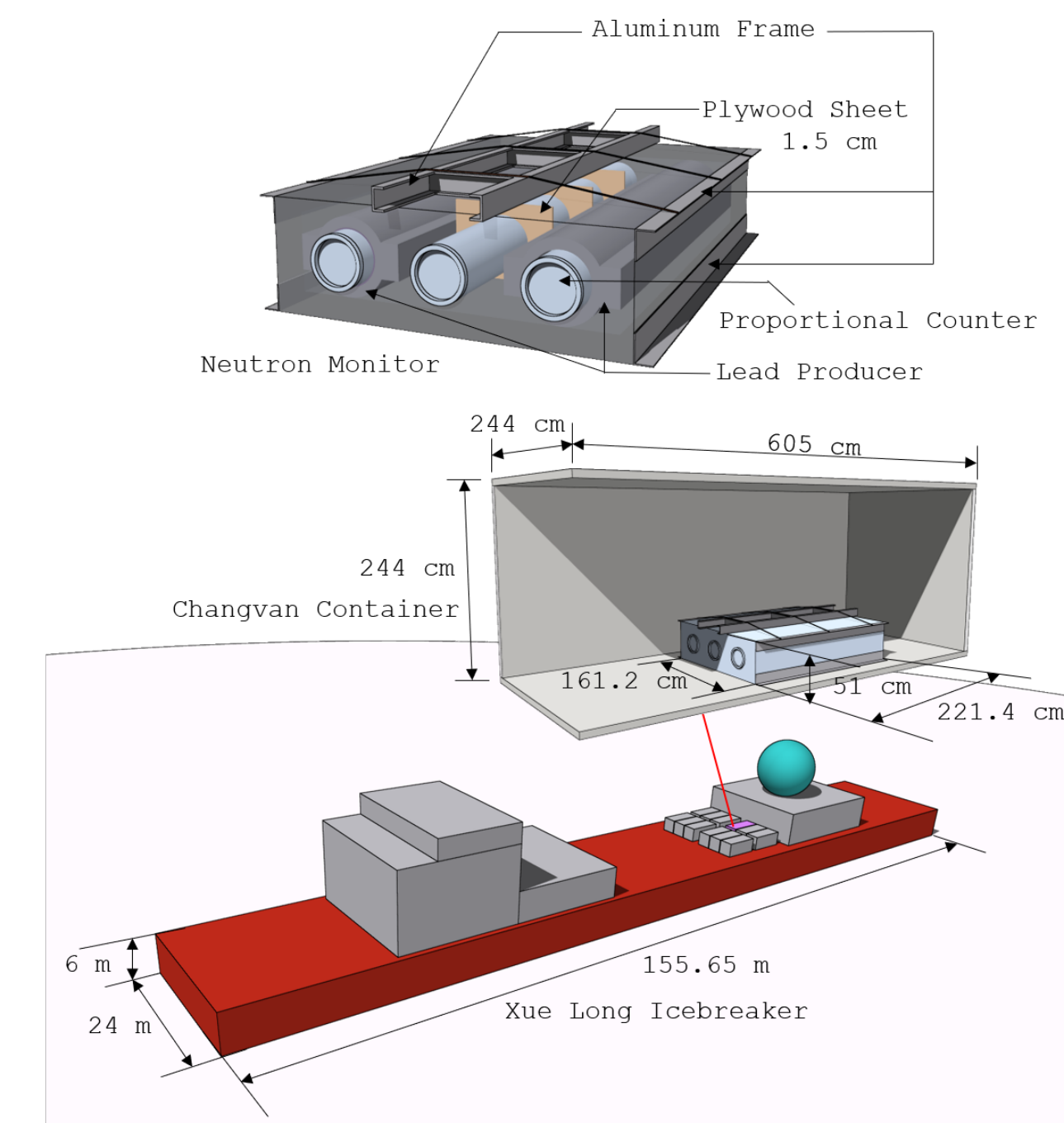

Figure 1: Changvan neutron monitor consists of 2 NM64s (with the lead producer) and an unleaded counter in the middle. Changvan was installed in an insulated shipping container and placed on the *Xuelong* icebreaker. This geometry is used in detector simulations. The renderings are created by Flair 3.1 [8]
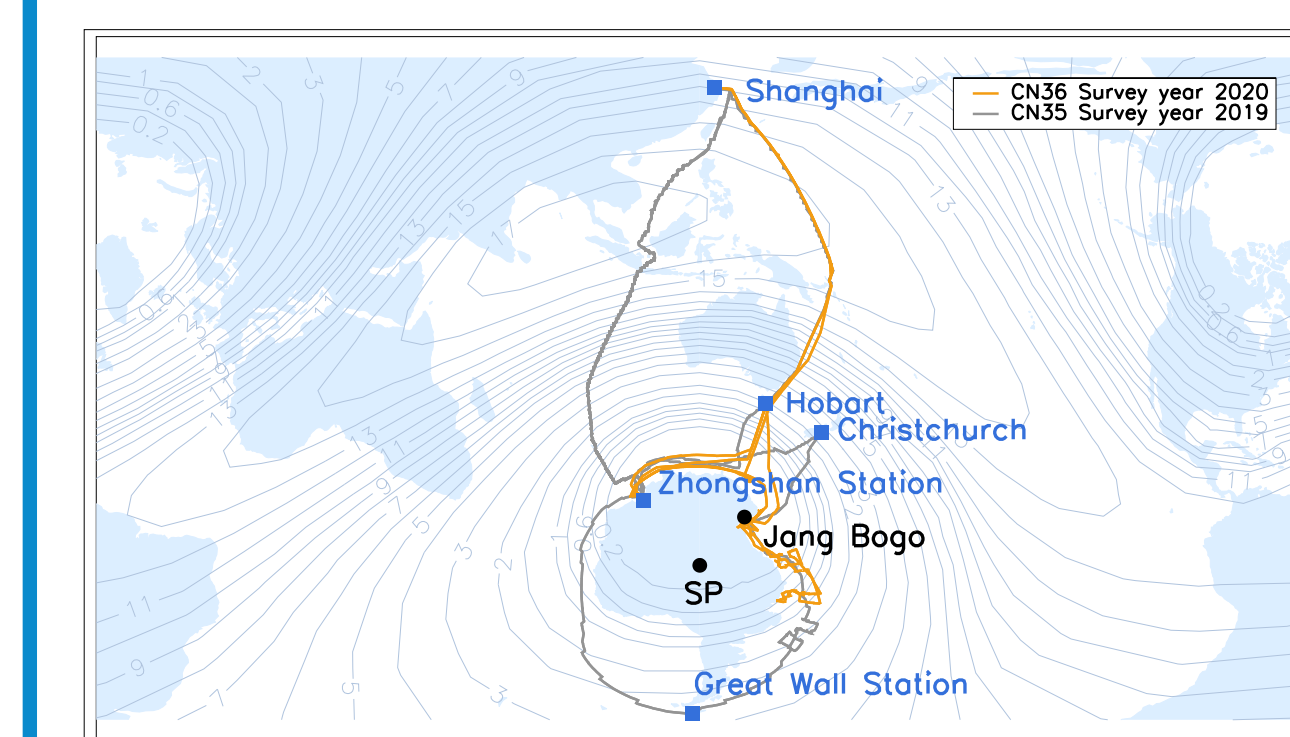
LATITUDE SURVEYS DURING 2019 – 2020

Figure 2: Path of Changvan neutron monitor in the 2019 (CN35: grey line) and 2020 (CN36: orange line) survey years. The contours with numbers indicate vertical cutoff rigidity (in the units of GV), calculated for February 11, 2019, at 12:00 UT.

During the 2019 and 2020 survey years, the Changvan was carried by the icebreaker *Xuelong* conducted by the Polar Research Institute of China (PRIC). The "survey year" refers to the year in which the voyage ended. The 2019 survey year covers the voyage from November 2, 2018 to March 11, 2019, and 2020 survey year covers the voyage from October 21, 2019 to April 22, 2020. The 2019 survey year is termed the 35 Chinese Antarctic Research Expedition (CN35), and the 2020 survey year is called CN36.

DATA

Data were acquired with the standard acquisition system used in 13 surveys during 1994–2007 [9]. The counting rate of each detector was recorded once per second together with the attitude of the ship (pitch and roll). Once per minute, the barometric pressure was recorded, as was the ship's position derived from GPS data. Apparent geomagnetic cutoffs [10, 11, 12] were calculated at one hour interval. We only have data for the second half of the 2019 survey year (from February 11 to March 11, 2019). Because of a heavy load of other shipping containers on CN35, we could not operate the Changvan on the voyage from Shanghai down to the Zhongshan station, a Chinese research station in Antarctica. In comparison, we have full data for the 2020 survey year (from October 21, 2019, to April 22, 2020). As we have more data in the subsequent survey year, we will only compare the simulation results with the results from that survey year. Here we used measured count rate vs. cutoff rigidity (P_c) from Yakum et al. (in preparation).

SIMULATION INFORMATION

Simulation information can be found in the table below:

	Type	No. of simulated particles
Atmospheric simulation	p	1,000,000
	α	1,000,000
Library	n	136,508
	p	13,486
	$\mu^\pm$	1,149,070
Detector simulation	n	100,000,000
	p	100,000,000
	μ	25,000,000

Simulation results were analyzed to obtained Yield Function, Count rate as cutoff rigidity and the ratios of the count rate.

COUNT RATES VS. CUTOFF RIGIDITY

We estimated the primary GCR spectrum above the atmosphere from the Local Interstellar spectrum (LIS), corresponding to [19] with a solar modulation $\phi = 426$ MV, as calculated from [18] to obtain count rates from simulations for individual tubes, shown in Figure 4. Here, T2 is the unleaded detector at the center, while T1 and T3 are leaded detectors flanking side of the middle tube. Both simulation and data were corrected to a mean sea level pressure at $P_0 = 760$ mmHg using $C_p = Ce^{\beta(P-P_0)}$, where P is pressure, C is the count rate, and C_p is the count rate corrected for pressure variation. The barometric pressure coefficient β, in units of percent per mmHg, was empirically determined by [9] and depends on the cutoff rigidity P_c (in GV) as following $\beta = 1.006 - 0.01534P_c$ %/mmHg. Figure 4 (a) shows simulated count rates corrected for pressure, and Figure 4 (b) shows measured count rates corrected for pressure. Figure 4 (c) shows the ratio of the Simulation/Data count rate. We can see that the simulated count rates are overestimated for all rigidity bin (scale on the right shows numbers greater than 1).

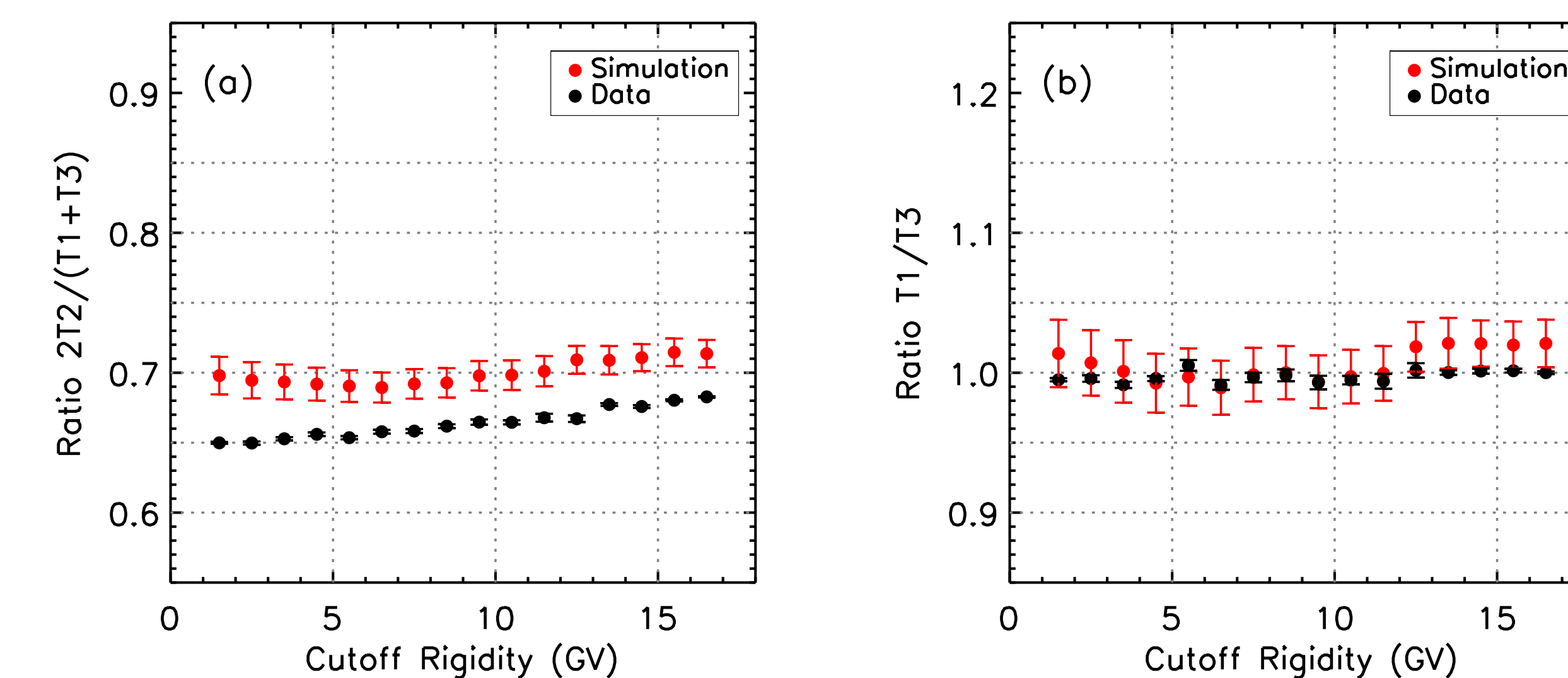## UNLEADED/LEADED COUNT RATE RATIOS VS. CUTOFF RIGIDITY

Figure 5: (a) The ratios of unleaded/leaded NM count rates. (b) The ratio of leaded/leaded NM rates. The vertical error bar represent the error propagation of the ratio, which still large for the simulated results.
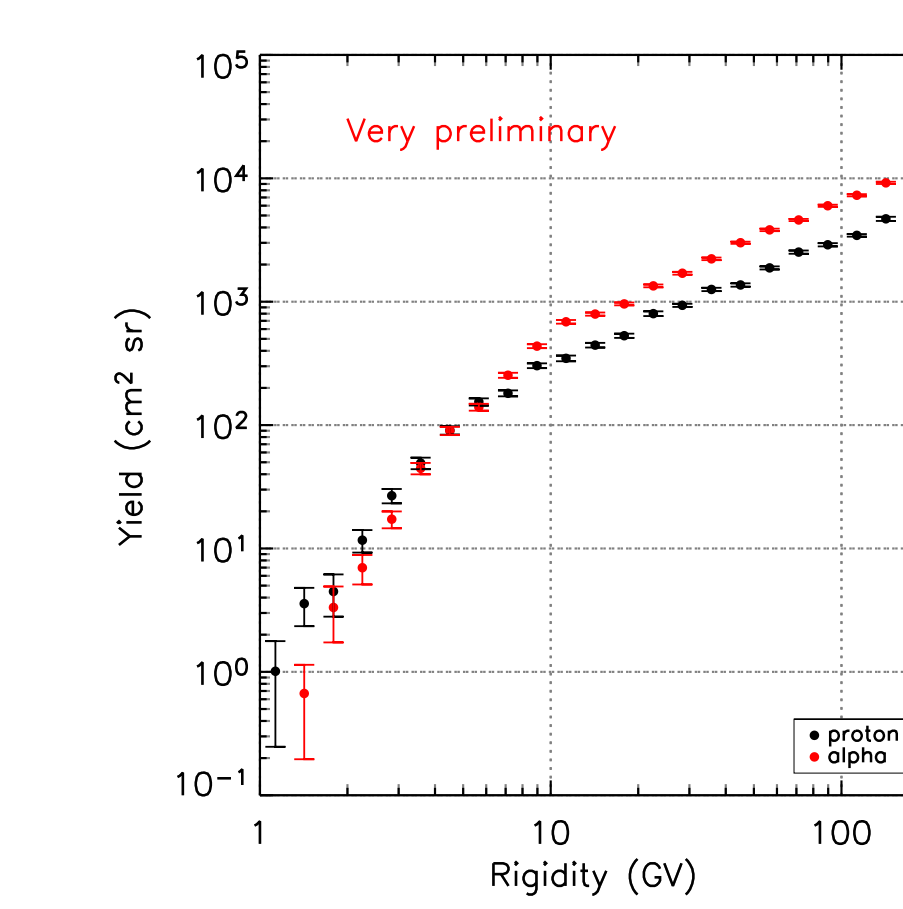
YIELD FUNCTION OF THE CHANGVAN MONITOR

Figure 3: Yield functions for protons and alphas of Changvan neutron monitor.

From these simulations we calculated yield function of the Changvan neutron monitor for primary protons and alphas, shown in Figure 3 We observe the crossover between alpha and proton yield functions at ∼3-4 GV. At high rigidity, the yield function for alphas is higher than that for protons by a factor of ∼2, roughly corresponding to the ratio of the total kinetic energy of an alpha and a proton at the same rigidity. The preliminary yields for alpha and proton seem reasonable, but we still need to do more simulations at lower rigidity than 6 GV for better statistics.
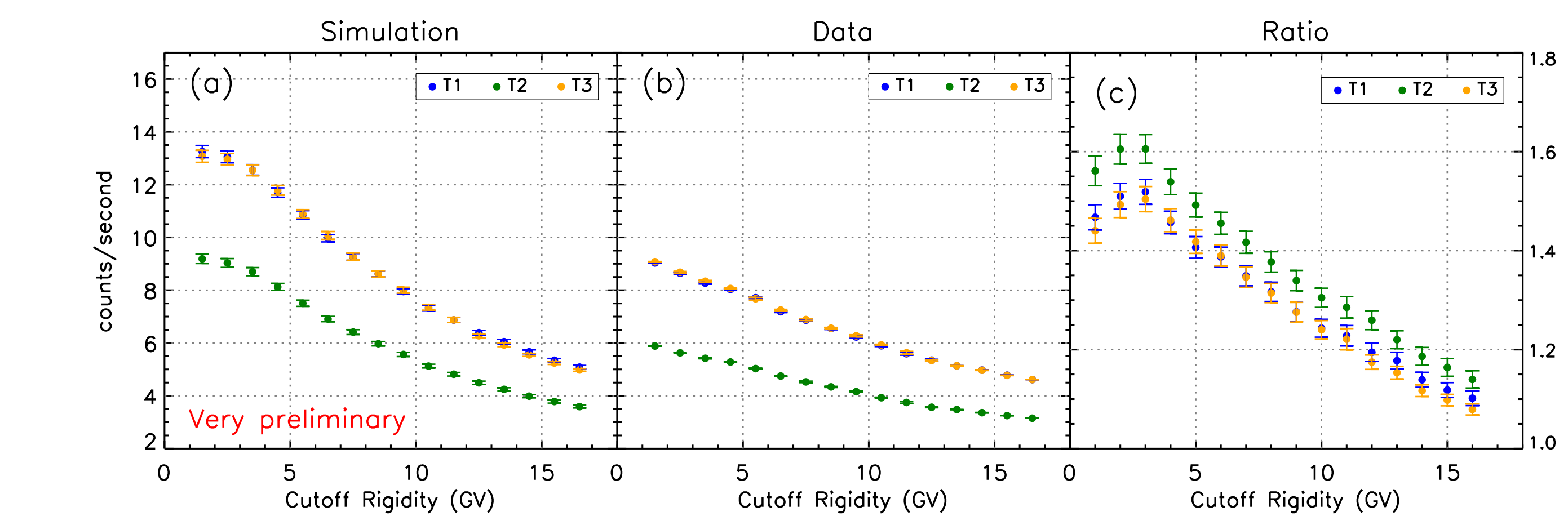

Figure 4: Comparison between (a) Simulation count rate and (b) Data count rate. The simulation count rate is higher than the Data count rate. The ratio of Simulation/Data count rate is provided in (c). The vertical error bar in (a)–(b) represents the standard error, and (c) the error propagation of the ratio; in many cases, the error bar is smaller than the plot symbol.

Such a Changvan semi-leaded 3NM64 can use the unleaded/leaded count rate ratio to determine the spectral index of relativistic solar ions with a single detector. Comparing simulation results for the ratio 2T2/(T1+T3) vs. cutoff rigidity to the actual ratio obtained from the latitude survey in Figure 5(a), we see that the simulated ratio was significantly higher than the actual count ratio across all cutoff rigidity ranges from 1-17 GV. The ratio T1/T3 vs. cutoff rigidity is near unity as expected.

We can clearly see that the ratio of the actual count rate depends on the cutoff rigidity with a nearly linear trend, while we do not see any trend in the simulation. At present, we cannot draw any conclusions regarding the obtained simulation result based on the Hobart atmosphere only. While conducting the actual experiment, the ship traveled through different atmospheres. In future work, we plan to modify some of the surrounding structures that affect the center unleaded tube more than the leaded tube and change the atmospheres corresponding to the actual observations. There is a very good agreement between the simulated and actual count rate ratio T1/T3. The size of the uncertainty propagation indicates that we need to do significantly more simulations to get statistically better results.

When we have a good result in Figure 4, it will lead us to obtain the comparable DRF to the actual result, and more precise yields for protons and alphas for further determination of the GCR spectrum.

ACKNOWLEDGEMENT